Appendix A.4 (report was formatted by HDSC)

Final Report

Production of Rainfall Frequency Grids for the Semiarid Southwest And Ohio River Basin Using an Optimized PRISM System

Prepared for
National Weather Service, Hydrologic Design Service Center
Silver Spring, Maryland

Prepared by
Christopher Daly and George Taylor
Spatial Climate Analysis Service
Oregon State University
Corvallis, Oregon

July 2004

Overall Project Goal

The contractor, Spatial Climate Analysis Service (SCAS) at Oregon State University (OSU), will produce a series of grids for rainfall frequency estimation using an optimized system based on the Parameter-elevation Regressions on Independent Slopes Model (PRISM) and HDSC-calculated point estimates for the Semiarid Southwest (SA) and Ohio River Basin (ORB) study domains. It is anticipated that successful progress on this task will lead to additional work of the same nature for the remainder of the United States including Puerto Rico and the Virgin Islands.

This Report

This report describes work performed to produce final index flood grids for 14 precipitation durations, ranging from 60 minutes to 60 days, for the SA and ORB regions.

Adapting the PRISM system

The PRISM modeling system was adapted for use in this project after an investigation was performed for the SA region. The same PRISM system was applied to the ORB region.

PRISM (Parameter-elevation Regressions on Independent Slopes Model) is a knowledge-based system that uses point data, a digital elevation model (DEM), and many other geographic data sets to generate gridded estimates of climatic parameters (Daly et al. ,1994; Daly et al., 2001; Daly et al., 2002) at monthly to daily time scales. Originally developed for precipitation estimation, PRISM has been generalized and applied successfully to temperature, among other parameters. PRISM has been used extensively to map precipitation, dew point, and minimum and maximum temperature over the

United States, Canada, China, and other countries. Details on PRISM formulation can be found in Daly et al. (2002) and Daly (2002).

Examples of PRISM products already produced for the United States include: (1) a new US climate atlas that includes monthly and annual average climate maps for precipitation, temperature, snowfall, degree days, and other parameters for the 1961-1990 period (Plantico et al., 2000); (2) sequential monthly maps for precipitation and mean maximum and minimum temperature for the period 1895-1997 (Daly et al., 2001); (3) peer-reviewed 1961-1990 mean monthly precipitation maps, certified as the official maps of the USDA (USDA-NRCS, 1998; Daly and Johnson, 1999); and (4) an update of the 1961-1990 maps to the 1971-2000 climatological period.

Adapting the PRISM system for mapping precipitation frequencies required an approach slightly different than the standard modeling procedure. The amount of station data available to HDSC for precipitation frequency was much less than that available for high-quality precipitation maps, such as the peer-reviewed PRISM 1961-1990 mean precipitation maps (USDA-NRCS, 1998). Data sources suitable for long-term mean precipitation but not for precipitation frequency included snow courses, short-term COOP stations, remote storage gauges, and others. In addition, data for precipitation durations of less than 24 hours are available from hourly rainfall stations only. This meant that mapping precipitation frequency using HDSC stations would sacrifice a significant amount of the spatial detail present in the 1961-1990 mean precipitation maps.

A pilot project to identify ways of capturing more spatial detail in the precipitation frequency maps was undertaken. Early tests showed that mean annual precipitation (MAP) was an excellent predictor of precipitation frequency in a local area, much better than elevation, which is typically used as the underlying, gridded predictor variable in PRISM applications. In these tests, the DEM, the predictor grid in PRISM, was replaced by the official USDA digital map of MAP for the lower 48 states (USDA-NRCS, 1998; Daly et al., 2001; Figure 1). Detailed information on the creation of the USDA PRISM precipitation grids is available from Daly and Johnson (1999). Figures 2 and 3 illustrate the superior predictive capability of MAP over the DEM for locations in the southwestern US. The relationships between MAP and precipitation frequency were strong because much of the incorporation of the effects of various physiographic features on mean precipitation patterns had already been accomplished with the creation of the MAP grid from PRISM. Now, it was only a matter of relating precipitation frequency to mean total precipitation. Preliminary PRISM maps of 2-year and 100-year, 24-hour precipitation were made for the Semiarid Southwest and compared to hand-drawn HDSC maps of the same statistics. Differences were minimal, and mostly related to differences in station data used.

Further investigation found that the square-root transformation of MAP produced somewhat more linear, tighter and cleaner regression functions, and hence, more stable predictions, than the untransformed values; this transformation was incorporated into subsequent model applications. Square-root MAP was a good local predictor of not only for longer-duration precipitation frequency statistics, but for short-duration statistics, as well (Figures 4 and 5). Therefore, it was determined that a modified PRISM system that used square-root MAP as the predictive grid was suitable for producing high-quality precipitation frequency maps for this project.

PRISM Configuration and Operation

For application to the SA and ORB regions, PRISM consisted of a local moving-window, index flood vs. MAP regression function that interacts with an encoded knowledge base and inference engine (Daly et al., 2002). This knowledge base/inference engine is a series of rules, decisions and

calculations that set weights for the station data points entering the regression function. In general, a weighting function contains knowledge about an important relationship between the climate field and a geographic or meteorological factor. The inference engine sets values for input parameters by using default values, or it may use the regression function to infer grid cell-specific parameter settings for the situation at hand. PRISM acquires knowledge through assimilation of station data, spatial data sets such as MAP and others, and a control file containing parameter settings.

The other center of knowledge and inference is that of the user. The user accesses literature, previously published maps, spatial data sets, and a graphical user interface to guide the model application. One of the most important roles of the user is to form expectations for the modeled climatic patterns, i.e., what is deemed "reasonable." Based on knowledgeable expectations, the user selects the station weighting algorithms to be used and determines whether any parameters should be changed from their default values. Through the graphical user interface, the user can click on any grid cell, run the model with a given set of algorithms and parameter settings, view the results graphically, and access a traceback of the decisions and calculations leading to the model prediction.

The moving-window regression function for index flood vs. MAP took the form

$$\text{Index flood value} = \beta_1 * \text{sqrt(MAP)} + \beta_0 \qquad (1)$$

where β_1 is the slope and β_0 is the intercept of the regression equation, and MAP is the grid cell value of 1961-90 mean annual precipitation

Upon entering the regression function for a given pixel, each station is assigned a weight that is based on several factors. In applications using a climate grid such as MAP as the predictor, the combined weight of a station is typically a function of distance, MAP, cluster, topographic facet, and coastal proximity, respectively. The combined weight W of a station is a function of the following:

$$W = f\{ W_d, W_z, W_c, W_f, W_p \} \qquad (2)$$

where W_d, W_z, W_c, W_f, and W_p are the distance, MAP, cluster, topographic facet, and coastal proximity, respectively. Distance, MAP, and cluster weighting are relatively straightforward in concept. A station is down-weighted when it is relatively distant or has a much different MAP value than the target grid cell, or when it is clustered with other stations (which leads to over-representation). Facet weighting effectively groups stations into individual hillslopes (or facets), at a variety of scales, to account for sharp changes in climate regime that can occur across facet boundaries. Coastal proximity weighting is used to define gradients in precipitation that may occur due to proximity to large water bodies (Daly et al., 1997; Daly and Johnson, 1999; Daly et al., 2002, 2003). No coastal areas were present in the SA region, precluding the need for coastal proximity. However, coastal proximity weighting was implemented in the ORB, which encompasses a large section of the eastern coastline. Shown in Figure 6, the coastal proximity grid is a measure of the distance from each pixel to the coastline, expressed in 10-km bands out to 90 km. The "coastline" is defined as the boundary between land and the ocean or Great Lakes. It does not include bays and inlets, such as Chesapeake Bay.

An example of the usefulness of coastal proximity weighting is shown in Figure 7. In this example of the 1-hour index flood precipitation vs mean annual precipitation (sqrt(MAP)) near Charleston, SC, coastal proximity weighting allowed the regression function to preserve higher 1-hour precipitation values along the immediate coastline by producing different regression functions at coastal and inland

pixels. In contrast, lack of coastal proximity weighting would produce similar regression functions for both pixels and would not recognize the coastal precipitation maximum.

Relevant PRISM parameters for the applications to 1- and 24-hour index flood statistics are listed in Tables 1 and 2. Further explanations of these parameters and associated equations are available in Daly (2002) and Daly et al. (2002). The difference to note between the parameter set in Tables 1 and 2 and that in Daly et al. (2002) is that the elevation weighting parameters in Daly et al. (2002) are now referred to here as MAP weighting parameters. This is because MAP, rather than elevation, is used as the predictor variable. The input parameters used for the 1-hour index flood application were generally applied to durations of 1-12 hours. The 24-hour input parameters were generally applied to durations of 24 hours and greater.

The values of radius of influence (R), the minimum number of on-facet (s_f) and total (s_t) stations required in the regression were based on information from user assessment via the PRISM graphical user interface, and on a jackknife cross-validation exercise, in which each station was deleted from the data set one at a time, a prediction made in its absence, and mean absolute error statistics compiled. One parameter that was varied significantly between the 1-hour (and up through 12 hours) and 24-hour (and up through 60 days) index flood applications was the minimum number of on-facet stations required in the regression (s_f; Tables 1 and2). PRISM has access to topographic facet grids at six different scales, from small-scale to large-scale (Daly et al., 2002). When developing each pixel's regression function, PRISM preferentially searches for stations on the same topographic facet as that of the target pixel, starting with the smallest-scale facet grid. If it does not find the minimum number of on-facet stations required, it moves to the next-larger-scale grid, and accumulates more stations, until either s_f is reached, or the largest-scale grid is used. Because the number of stations available for 1-hour – 12-hour index flood mapping was so much smaller than that for 24-hour – 60-day mapping, a much lower s_f threshold for on-facet stations was used; this kept the applications for the two groups of durations using about the same scale of facet grids in station selection and promoted consistency among the two applications.

Input parameters that changed readily among the various durations were the minimum allowable slope (β_{1m}) and default slope (β_{1d}) of the regression function, with the maximum allowable slope (β_{1x}) varying less readily. Slopes are expressed in units that are normalized by the average observed value of the precipitation in the regression data set for the target cell. Evidence gathered during model development indicates that this method of expression is relatively stable in both space and time (Daly et al., 1994).

Bounds are put on the slopes to minimize unreasonable slopes that might occasionally be generated due to local station data patterns; if the slope is out of bounds and cannot be brought within bounds by the PRISM outlier deletion algorithm, the default slope is invoked (Daly et al., 2002). Slope bounds and default values were based on PRISM diagnostics that provided information on the distribution of slopes across the modeling region. The default value was set to approximate the average regression slope calculated by PRISM. The upper and lower bounds were set to approximately the 95th and 5th percentiles of the distribution of slopes, respectively, because many of the slopes outside this range are typically found to be questionable. For these applications, slope bounds typically increased with increasing duration (Table 3). In general, the longer the duration, the larger the slope bounds. This is primarily a result of higher precipitation amounts at the longer durations, and the tendency for longer-duration index flood statistics to bear a stronger and steeper relationship with MAP than shorter-durations statistics.

One relatively new PRISM input parameter not discussed in Daly et al. (2002) is D_m, the minimum allowable distance in the distance weighting function (Tables 1 and 2). Any station falling within D_m of the target pixel is set to a distance of D_m. D_m was implemented in the ORB (only) with a value of 50 km because it was recognized that many small-scale spatial features (bulls eyes) in the MAP grid, especially in flat terrain, may have not reflected actual climate features, but variations in station data completeness and period of record. The effect of implementing D_m was to spatially smooth the relationship between MAP and index flood over a larger area and produce more spatially homogeneous results. This restriction was applied to all parts of the ORB, except coastal areas, where a rapidly-changing relationship between MAP and index flood produced realistic small-scale features along the coastal strip. When such a smoothing effect is applied, the maps do not reflect the actual station precipitation values quite as closely. Figure 8 shows how well the interpolated grid cell values reproduced the actual station precipitation used in the mapping for 1-hour and 24-hour index flood statistics, with and without the 50-km distance limitation. The correlation coefficient between observed and gridded precipitation fell from 0.91 to 0.81 when the limitation was applied to the 1-hour statistic, and dropped from 0.95 to 0.91 when applied to the 24-hour statistic. The drop in correlation became progressively less pronounced at the longer durations.

After completion of the SA mapping and during the ORB mapping, updates of the 1961-1990 MAP grids to the 1971-2000 climatological period became available. The 1971-2000 grid was created using 1961-1990 MAP as the predictor grid. There are only subtle differences between the two MAP grids, but it was decided that the ORB mapping should use the latest MAP grid. Therefore, the SA maps reflect the 1961-1990 MAP predictor grid and the ORB maps reflect the 1971-2000 predictor grid.

Results

PRISM cross-validation statistics for 1- and 24-hour applications to the SA and ORB regions were compiled and summarized in Tables 4 and 5. In the SA, overall bias was less than 2 percent, and mean absolute error was about 10 percent. In the ORB, errors were lower (about 0.5% bias and 6% mean absolute error), owing to less terrain complexity and higher station density. One-hour errors were somewhat higher than those for the 24-hour run. Likely reasons for this are the much smaller number of stations available, and the somewhat weaker relationship between 1-hour index flood and MAP, compared to those for the 24-hour index flood. Errors for 2- to 12-hour durations were similar to those for the 1-hour duration, and errors for 2 to 60-day durations were similar to those for the 24-hour duration. Overall, these errors are quite low, and are likely comparable to errors associated with precipitation measurement and the calculation of index flood statistics.

Stations used in the SA modeling applications are shown in Figure 9. During the initial modeling process, three stations were found to be unusual: two in the 1-hour application and one in the 24-hour application. The two unusual 1-hour stations were Independence, CA (04-4235), and Raton WB Airport, NM (29-7283). Independence had a 1-hour value that was much lower than other stations in the region; it was also low when compared to its 24-hour value. Subsequent analysis showed that this station had a relatively short period of record. Conversely, Raton WB Airport seemed too high, compared to its neighbors. Both stations were omitted from the final 1-hour index flood application. [Note: The stations met the criteria for the original precipitation frequency analysis and so were retained in the analysis conducted by HDSC and only omitted from the mapping process. - comment added by HDSC] Red Rock Canyon, NV (26-6691) appeared unusual during the modeling of the 24-hour index flood. It is sited on the southern flank of the Spring Mountains, just northwest of Las Vegas. This is an area of steep elevation, and hence, precipitation, gradients. The Red Rock Canyon 24-hour index flood value seemed high compared to the underlying MAP grid-cell value; however,

subsequent analysis showed that the underlying MAP grid value was higher than the stations' actual MAP, indicating that imprecision in either the station location or the 4-km grid cell resolution caused a misalignment between the grid MAP and station MAP. This problem was alleviated by substituting the station's MAP value for the grid MAP value when calculating the moving-window regression function.

Stations used in the ORB modeling applications are shown in Figure 10. During the review process, several bulls eyes were identified and questioned. One was found to be caused by a suspicious index flood station value, while the others were caused by unusual spots on the MAP predictor grid, which in turn were caused by unusual station averages used during the mapping of the 1961-1990 and 1971-2000 MAP grids. One suspicious station was Wateree Dam, SC (38-8979), which had an unusually low 1-hour index flood value. This was also noticed by the South Carolina State Climatologist after the original MAP mapping was completed (unfortunately). It was felt that because it is located at a dam, convective precipitation could be suppressed due to proximity to water. The MAP grid was altered to remove the effects of this station. Adding the 50-km minimum distance criterion mitigated its direct effect on the index flood grids, so the station was retained in the mapping process. Tangier Island, VA (44-8323), in Chesapeake Bay, produced a low area in the MAP grid, which was propagated to surrounding areas. It is possible that its location on an island suppressed convective precipitation, and thus lowered the MAP, but no conclusive evidence was presented. The MAP grid was altered to reduce the severity of the bulls eye. Manassas, VA (44-5213), and Middlebourne, OH (33-5199), also produced low spots in the MAP grid. The MAP grid was altered to reduce the severity of these bulls eyes.

After initial mapping of the ORB, three stations were found to have gridded index flood values that were significantly different than their station point values: Tuckasegee (31-8754), Mt. Mitchell (31-5921), and Parker (31-6565), NC. All three were located in the southern Appalachians, an area of steep elevation, and hence, precipitation, gradients, indicating that imprecisions in either the station location or the 4-km grid cell resolution caused a misalignment between the grid MAP and station MAP. This problem was alleviated by moving the station locations slightly.

Draft grids of 1- and 24-hour index flood statistics for the SA and ORB regions were produced by running PRISM at 2.5-minute (~4-km) resolution. These grids were reviewed by HDSC personnel, and found to be suitable for review by the larger user community, after some revision. A full set of maps for all index flood durations was then produced, including 1, 2, 3, 6, 12, and 24 hours; and 2, 4, 7, 10, 20, 30, 45, and 60 days. The maps were subjected to pixel-by-pixel tests to ensure that shorter duration values did not exceed those of longer duration values. To make the grids presentable for detailed contour plotting, SCAS used a Gaussian filter to resample the grids to 30-sec (~ 1km) resolution. Sample final filtered grids are shown in Figures 11-14. These grids were delivered electronically to HDSC via ftp.

References

Daly, C., 2002: Variable influence of terrain on precipitation patterns: Delineation and use of effective terrain height in PRISM. *World Wide Web document*. http://www.ocs.orst.edu/pub/prism/docs/effectiveterrain-daly.pdf

_____, E.H. Helmer, and M. Quinones, 2003: Mapping the climate of Puerto Rico, Vieques, and Culebra. *International Journal of Climatology*, **23**, 1359-1381.

_____ and G.L. Johnson, 1999: PRISM spatial climate layers: their development and use. *Short Course on Topics in Applied Climatology, 79th Annual Meeting of the American Meteorological Society,* 10-15 January, Dallas, TX. 49 pp. http://www.ocs.orst.edu/pub/prism/docs/prisguid.pdf

_____, R.P. Neilson, and D.L. Phillips, 1994: A Statistical-Topographic Model for Mapping Climatological Precipitation over Mountainous Terrain. *J. Appl. Meteor*. **33**, 140-158.

_____, G. Taylor, and W. Gibson, 1997: The PRISM Approach to Mapping Precipitation and Temperature, 10th Conf. on Applied Climatology, Reno,NV, *Amer. Meteor. Soc*., 10-12. http://www.ocs.orst.edu/pub/prism/docs/appclim97-prismapproach-daly.pdf

_____, G.H. Taylor, W. P. Gibson, T.W. Parzybok, G. L. Johnson, P. Pasteris, 2001: High-quality spatial climate data sets for the United States and beyond. *Transactions of the American Society of Agricultural Engineers* **43**, 1957-1962.

_____, W. P. Gibson, G.H. Taylor, G. L. Johnson, and P. Pasteris, 2002: A knowledge-based approach to the statistical mapping of climate. *Clim. Res*., **22**, 99-113. http://www.ocs.orst.edu/pub/prism/docs/climres02-kb_approach_statistical_mapping-daly.pdf

Plantico, M.S., L.A. Goss, C. Daly, and G. Taylor, 2000: A new U.S. climate atlas. In: *Proc., 12th AMS Conf. on Applied Climatology, Amer. Meteorological Soc*., Asheville, NC, May 8-11, 247-248.

USDA-NRCS, 1998: PRISM Climate Mapping Project--Precipitation. Mean monthly and annual precipitation digital files for the continental U.S. *USDA-NRCS National Cartography and Geospatial Center*, Ft. Worth TX. December, CD-ROM.

Table 1. Values of relevant PRISM parameters for modeling of 1- and 24-hour index flood statistics for the SA (semiarid southwest region). See Daly et al. (2002) for details on PRISM parameters.

Name	Description	1-hour/24-hour Values
Regression Function		
R	Radius of influence	60/70 km*
s_f	Minimum number of on-facet stations desired in regression	2/12 stations*
s_t	Minimum number of total stations desired in regression	20/20 stations*
β_{1m}	Minimum valid regression slope	1.0/2.0[+]
β_{1x}	Maximum valid regression slope	30.0/30.0[+]
β_{1d}	Default valid regression slope	3.5/5.9[+]
Distance Weighting		
A	Distance weighting exponent	2.0/2.0
F_d	Importance factor for distance weighting	0.5/0.5
D_m	Minimum allowable distance	0 km
MAP Weighting**		
B	MAP weighting exponent	1.0/1.0
F_z	Importance factor for MAP weighting	0.5/0.5
Δz_m	Minimum station-grid cell MAP difference below which MAP weighting is maximum	50/50%
Δz_x	Maximum station-grid cell MAP difference above which MAP weight is zero	500/500%
Facet Weighting		
C	Facet weighting exponent	0.5/0.5 [‡]
g_m	Minimum inter-cell elevation gradient, below which a cell is flat	1/1 m/cell
λ_x	Maximum DEM filtering wavelength for topographic facet determination	80/80 km
Coastal Proximity Weighting		
v	Coastal proximity weighting exponent	Not applied

* Optimized with cross-validation statistics (see Table 2).

[+] Slopes are expressed in units that are normalized by the average observed value of the precipitation in the regression data set for the target cell. Units here are 1/[sqrt(MAP(mm))*1000].

** Normally referred to as elevation weighting

[‡] Maximum value; actual value varied dynamically by the model.

Table 2. Values of relevant PRISM parameters for modeling of 1- and 24-hour index flood statistics for the ORB (Ohio River Basin). See Daly et al. (2002) for details on PRISM parameters.

Name	Description	1-hour/24-hour Values
Regression Function		
R	Radius of influence	60/70 km*
s_f	Minimum number of on-facet stations desired in regression	2/12 stations*
s_t	Minimum number of total stations desired in regression	20/20 stations*
β_{1m}	Minimum valid regression slope	0.6/1.2$^+$
β_{1x}	Maximum valid regression slope	30.0/30.0$^+$
β_{1d}	Default valid regression slope	3.5/5.9$^+$
Distance Weighting		
A	Distance weighting exponent	2.0/2.0
F_d	Importance factor for distance weighting	0.5/0.5
D_m	Minimum allowable distance	50/50 km
MAP Weighting**		
B	MAP weighting exponent	1.0/1.0
F_z	Importance factor for MAP weighting	0.5/0.5
Δz_m	Minimum station-grid cell MAP difference below which MAP weighting is maximum	50/50%
Δz_x	Maximum station-grid cell MAP difference above which MAP weight is zero	500/500%
Facet Weighting		
C	Facet weighting exponent	0.5/0.5 ‡
g_m	Minimum inter-cell elevation gradient, below which a cell is flat	1/1 m/cell
λ_x	Maximum DEM filtering wavelength for topographic facet determination	80/80 km
Coastal Proximity Weighting		
v	Coastal proximity weighting exponent	1.0/1.0‡

* Optimized with cross-validation statistics (see Table 4).

+ Slopes are expressed in units that are normalized by the average observed value of the precipitation in the regression data set for the target cell. Units here are 1/[sqrt(MAP(mm))*1000].

** Normally referred to as elevation weighting

‡ Maximum value; actual value varied dynamically by the model.

Table 3. Values of PRISM slope parameters for modeling of index flood statistics for the SA (Semiarid Southwest) and ORB (Ohio River Basin) for all durations. See Table 1 for definitions of parameters.

	Semiarid Southwest			Ohio River Basin		
Duration	β_{1m}	β_{1x}	β_{1d}	β_{1m}	β_{1x}	β_{1d}
1 hour	1.0	30.0	3.5	0.6	30.0	3.5
2 hour	1.2	30.0	3.8	0.7	30.0	3.8
3 hour	1.8	30.0	4.0	1.1	30.0	4.0
6 hour	2.0	30.0	4.5	1.2	30.0	4.5
12 hour	2.0	30.0	5.5	1.2	30.0	5.5
24 hour	2.0	30.0	5.9	1.2	30.0	5.9
48 hour	2.2	30.0	6.5	1.3	30.0	6.5
4 day	2.6	50.0	7.1	1.6	50.0	7.1
7 day	3.4	50.0	7.7	1.9	50.0	7.7
10 day	3.4	50.0	8.6	2.0	50.0	8.6
20 day	4.3	50.0	9.4	2.6	50.0	9.4
30 day	4.7	50.0	10.9	2.8	50.0	10.0
45 day	5.0	50.0	10.5	3.0	50.0	10.5
60 day	5.2	50.0	10.9	3.5	50.0	10.9

Table 4. PRISM cross-validation errors for 1- and 24-hour index flood applications to the SA (semiarid southwest) region.

Statistic	N	% Bias	% MAE
1-hour index flood	459	1.93	11.84
24-hour index flood	1822	1.56	8.99

Table 5. PRISM cross-validation errors for 1- and 24-hour index flood applications to the ORB (Ohio River Basin) region.

Statistic	N	% Bias	% MAE
1-hour index flood	946	0.48	5.77
24-hour index flood	2944	0.41	4.34

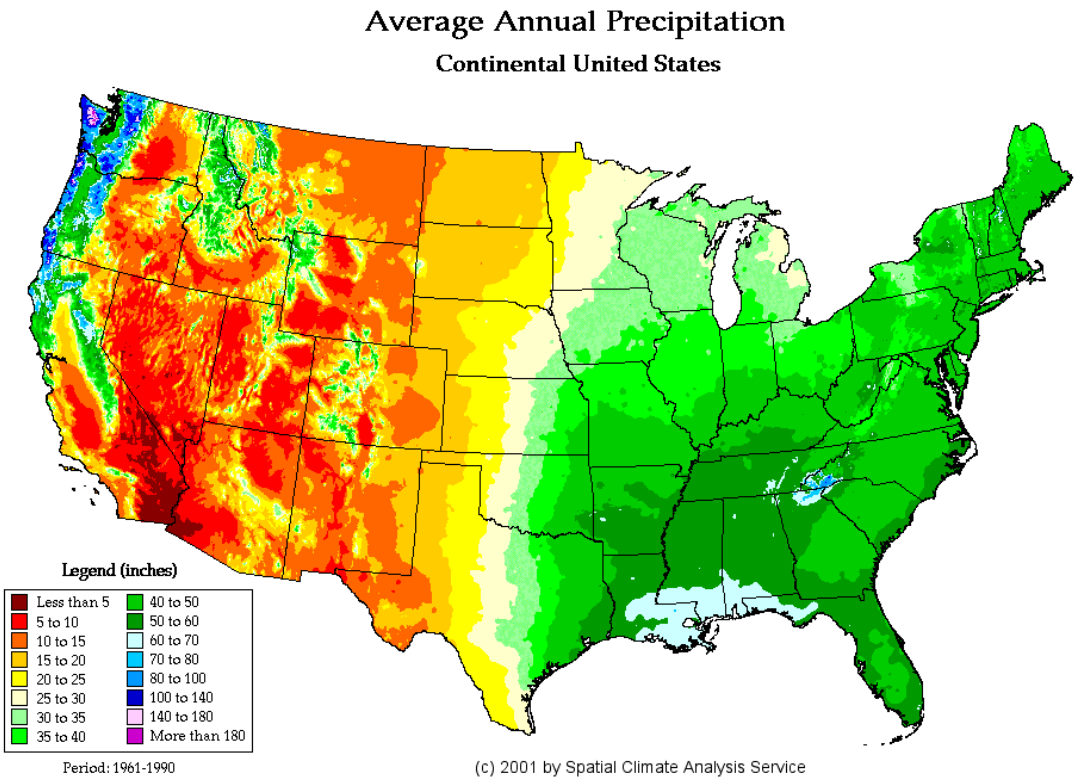

Figure 1. Grid of PRISM Mean Annual Precipitation for the United States (USDA-NRCS 1998, Daly and Johnson 1999), used as the spatial predictor of precipitation frequency.

(a)

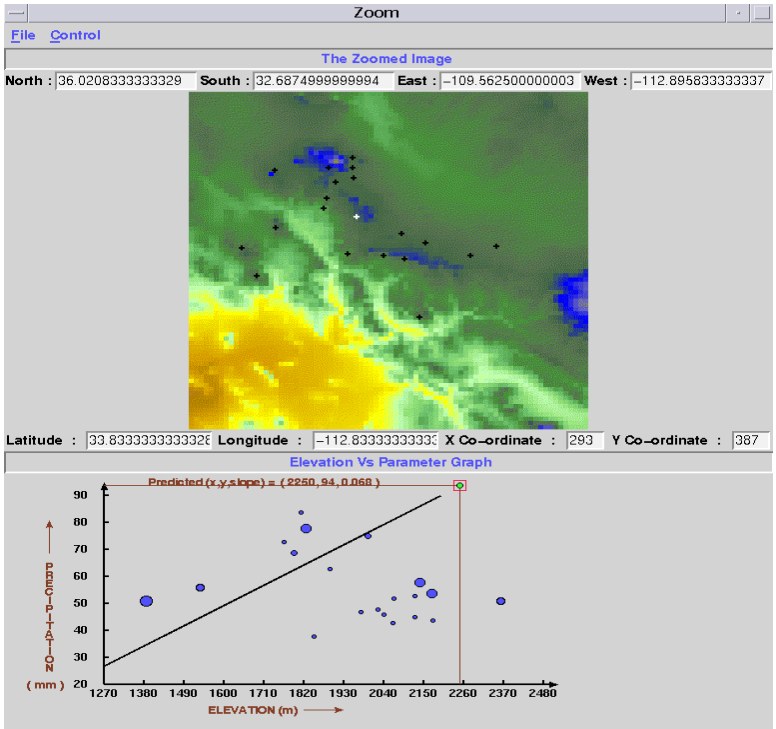

(b)

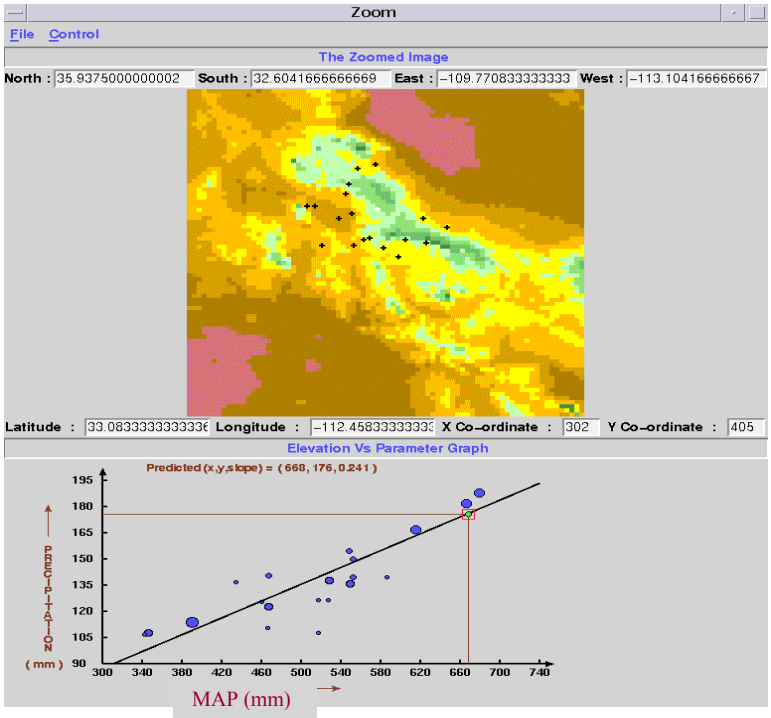

Figure 2. PRISM graphical user interface showing: (a) 100-yr 24-hour precipitation vs elevation; and (b) 100-yr 24-hour precipitation vs mean annual precipitation (MAP), Mogollon Rim, AZ. Size of dot indicates relative weight of station in regression function.

(a)

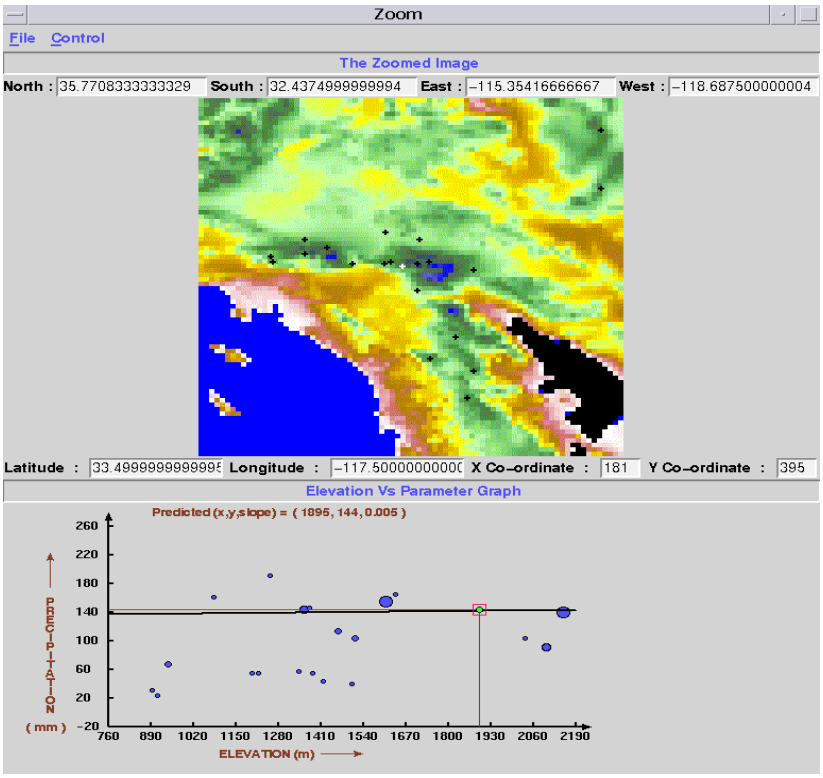

(b)

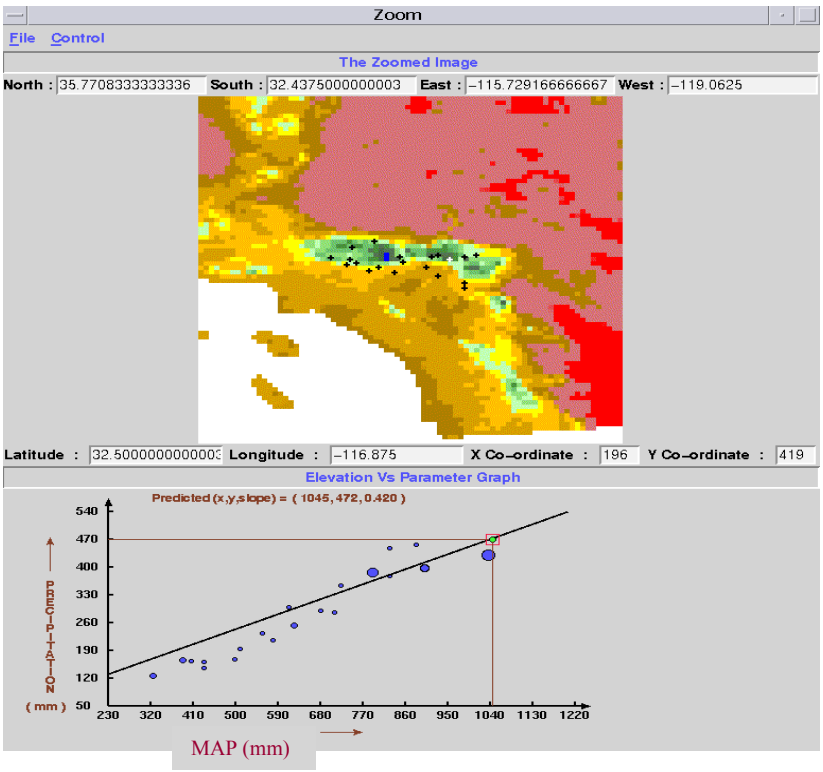

Figure 3. PRISM graphical user interface showing: (a) 100-yr 24-hour precipitation vs elevation; and (b) 100-yr 24-hour precipitation vs mean annual precipitation (MAP), San Bernardino Mountains, CA. Size of dot indicates relative weight of station in regression function.

(a)

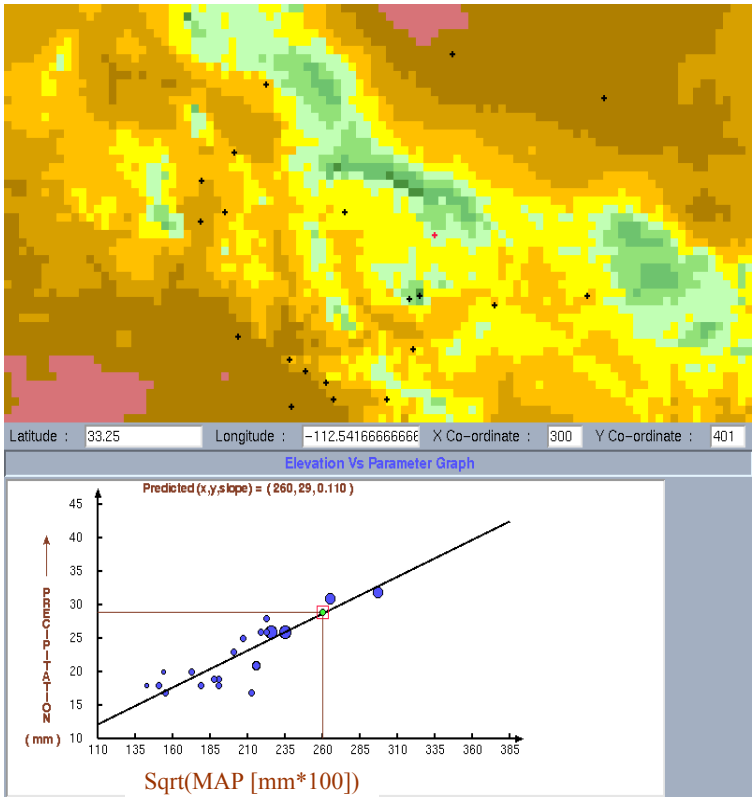

(b)

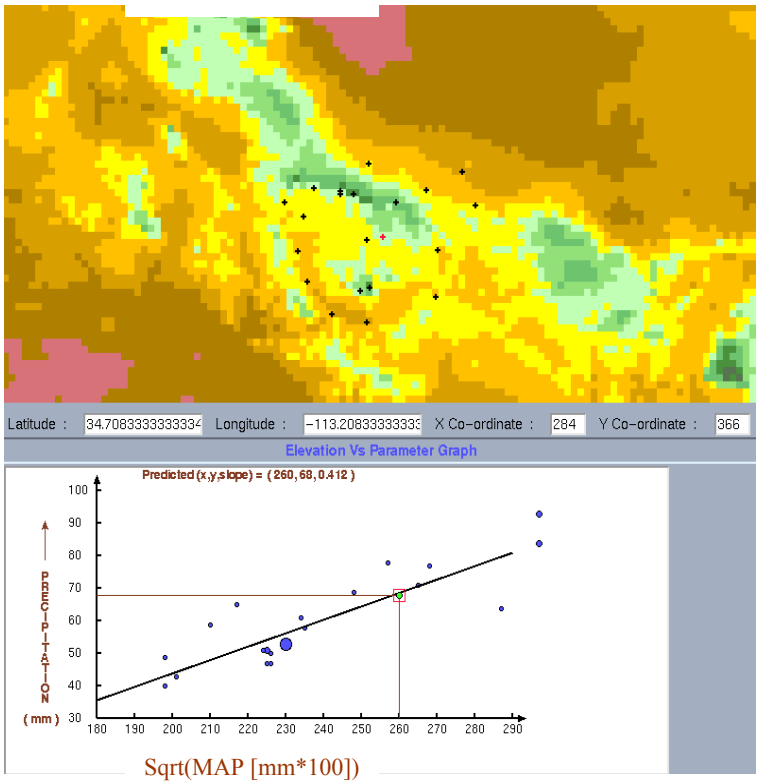

Figure 4. PRISM graphical user interface showing: (a) 1-hour index flood precipitation vs mean annual precipitation (sqrt(MAP)); and (b) 24-hour index flood precipitation vs sqrt(MAP), Mogollon Rim, AZ. Size of dot indicates relative weight of station in regression function.

(a)

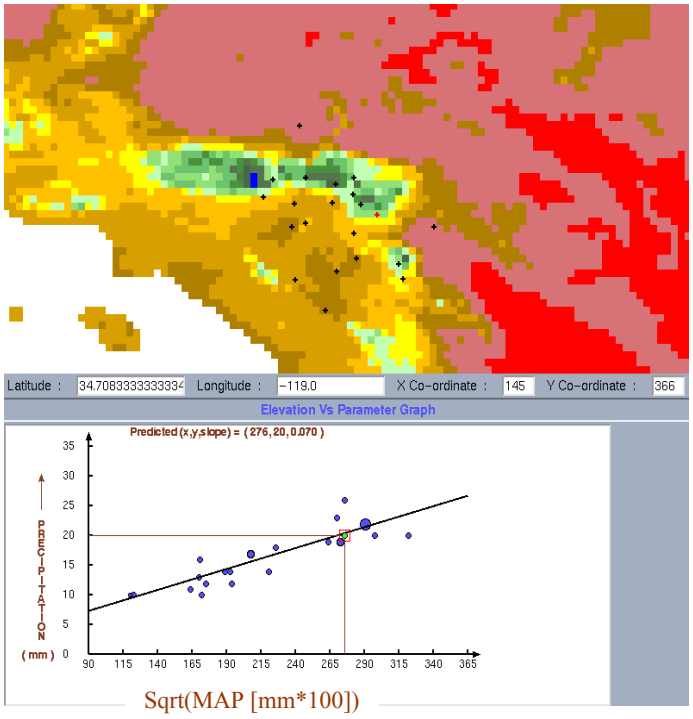

(b)

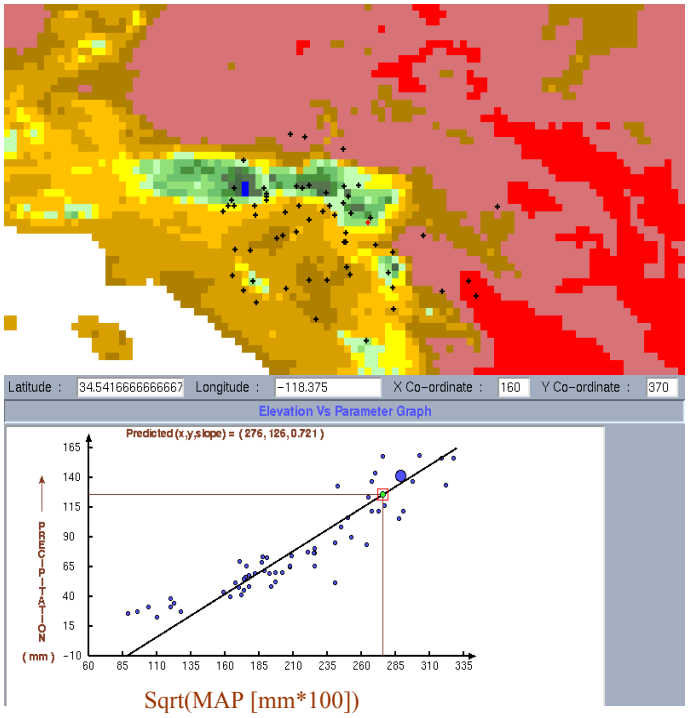

Figure 5. PRISM graphical user interface showing: (a) 1-hour index flood precipitation vs mean annual precipitation (sqrt(MAP)); and (b) 24-hour index flood precipitation vs sqrt(MAP), San Bernardino Mountains, CA. Size of dot indicates relative weight of station in regression function.

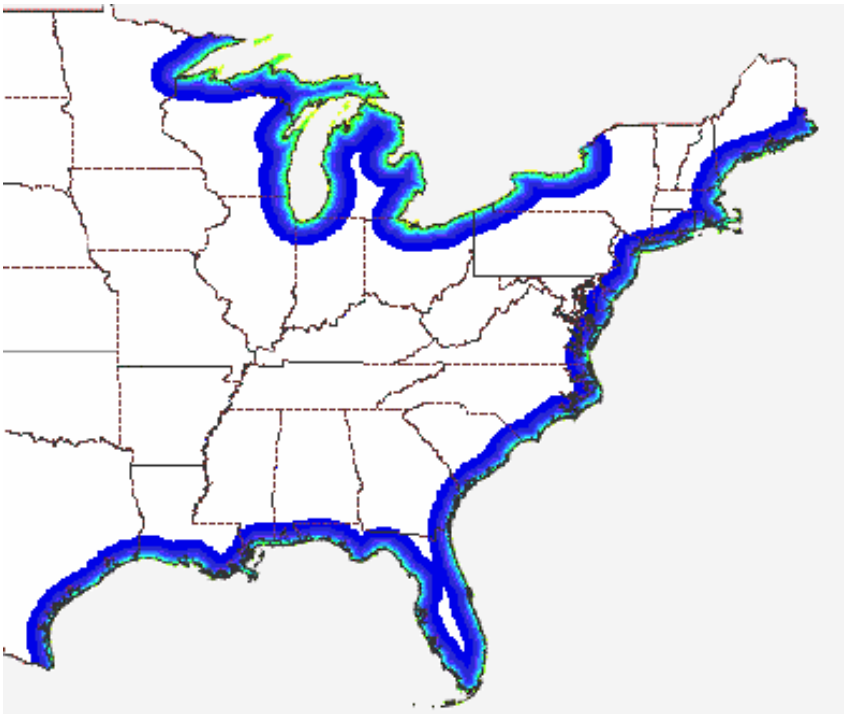

Figure 6. Coastal areas delineated in the eastern United States.

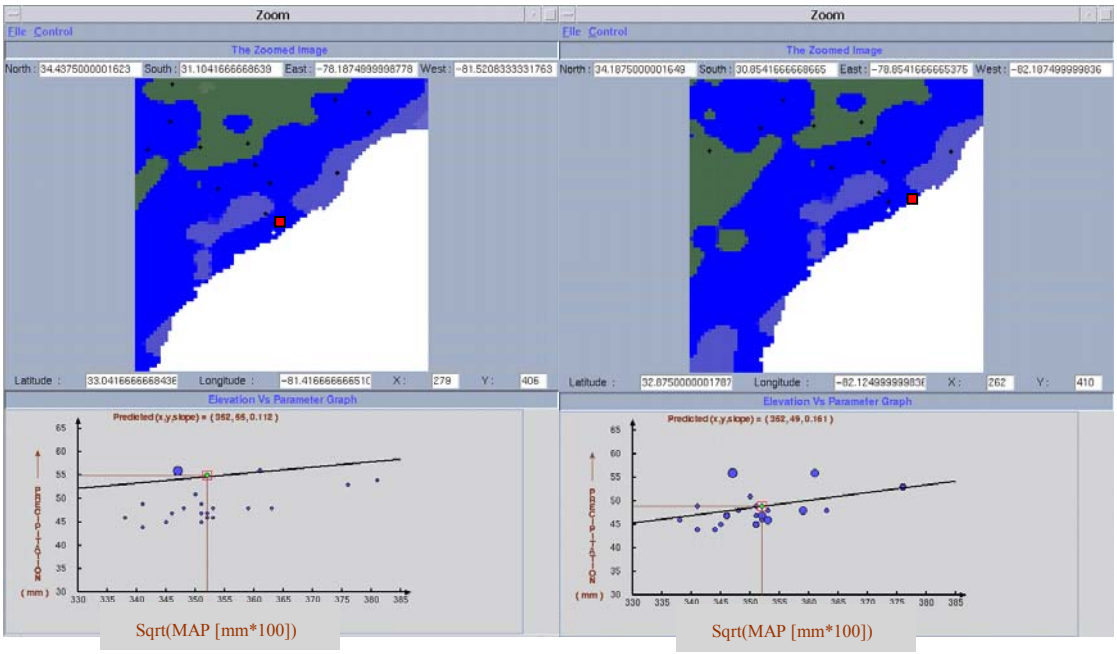

(a) Coastal pixel, coastal proximity enabled. (b) Coastal pixel, coastal proximity disabled.

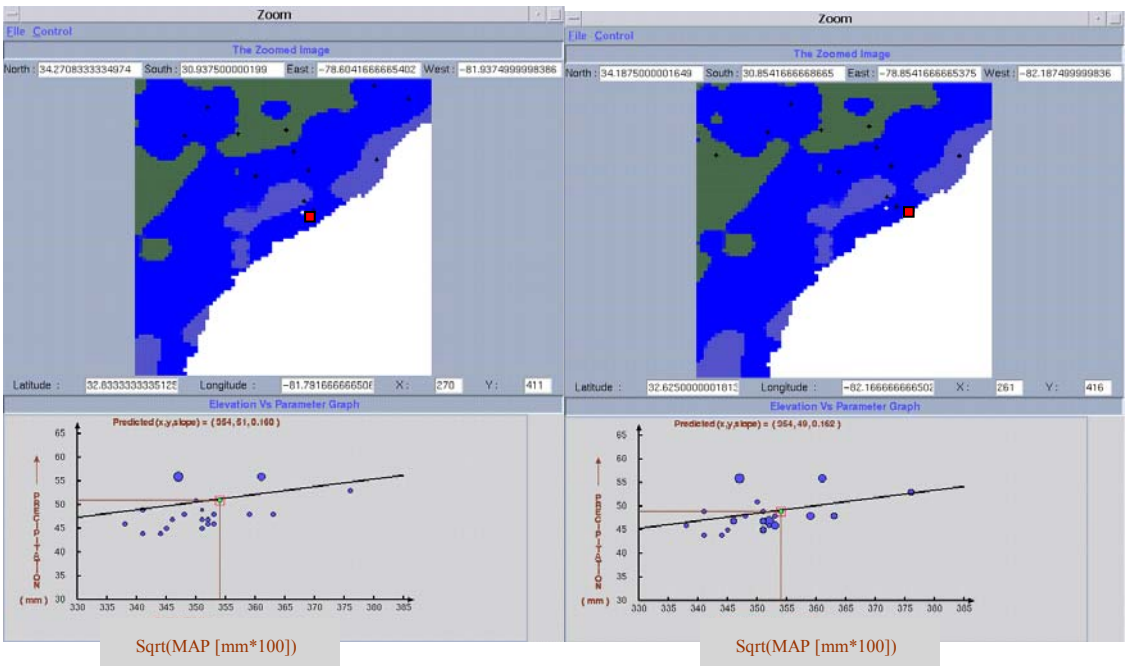

(c) Inland pixel, coastal proximity enabled. (d) Inland pixel, coastal proximity disabled.

Figure 7. PRISM graphical user interface showing 1-hour index flood precipitation vs mean annual precipitation (sqrt(MAP)) near Charleston, SC. Coastal proximity weighting allows the regression function to preserve higher 1-hour precipitation values along the immediate coastline by producing different regression functions at coastal and inland pixels. In contrast, lack of coastal proximity weighting produces similar regression functions for both pixels and does not recognize the coastal precipitation maximum. Target pixel is shown as a red square. Size of dot on scatterplot indicates relative weight of station in regression function.

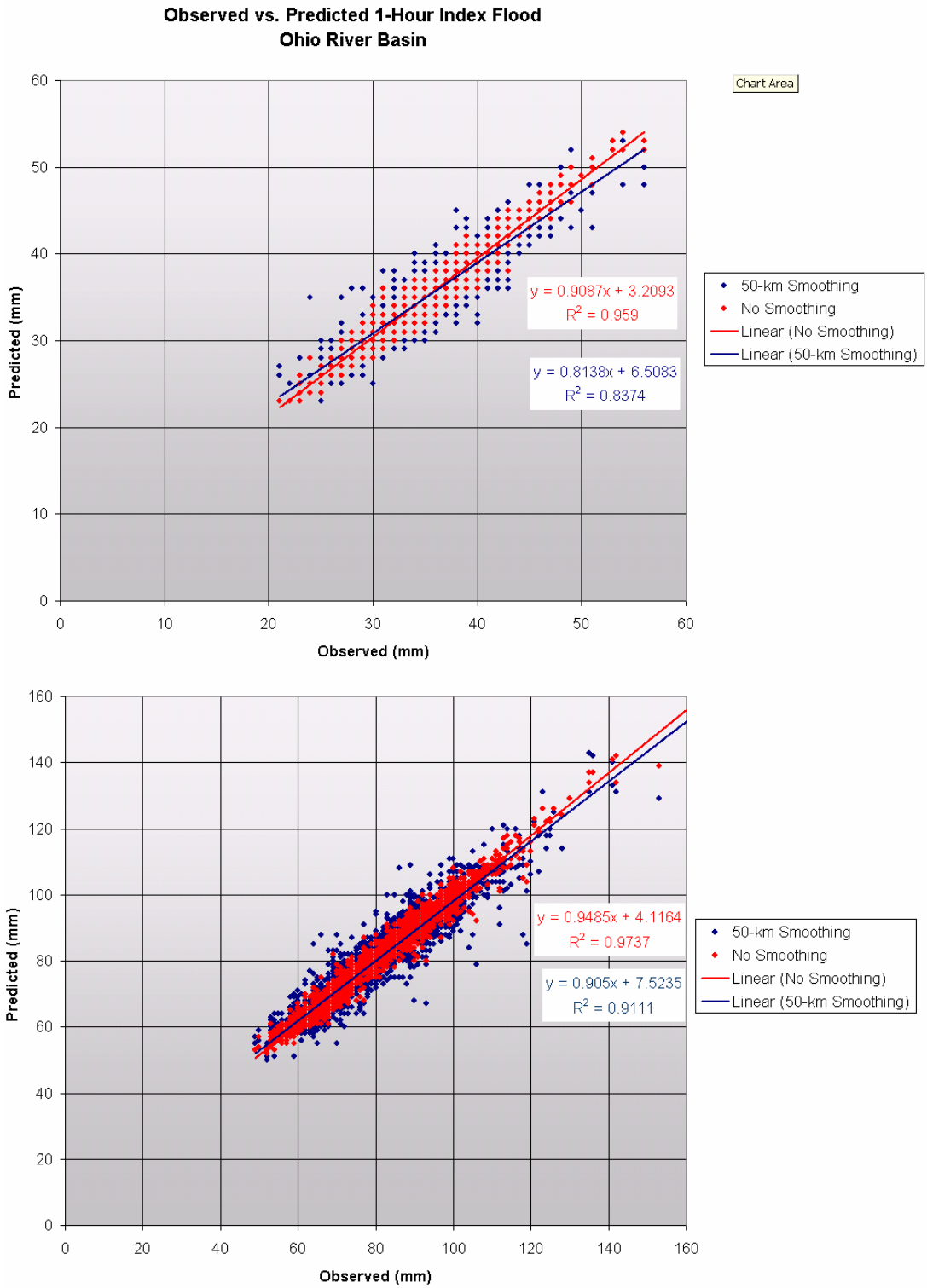

Figure 8. Relationships between station and gridded precipitation values for 1- and 24-hour index floods, with and without the 50-km distance weighting limitation (smoothing). See text for details.

(a)

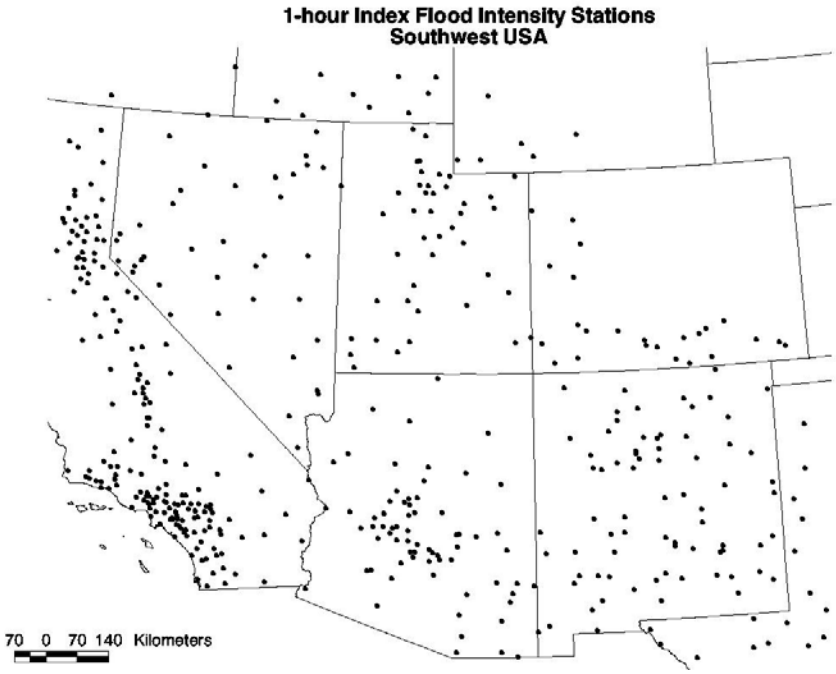

(b)

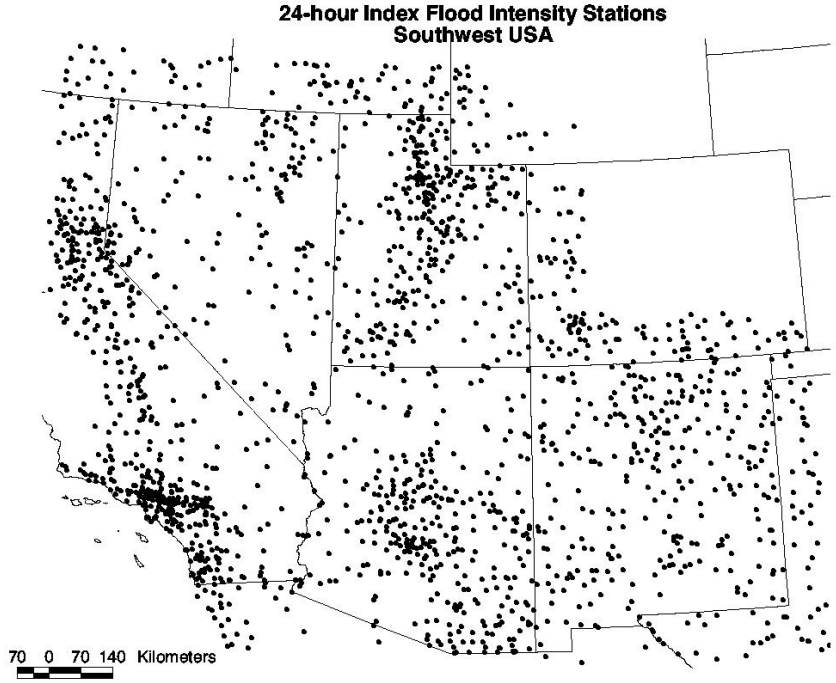

Figure 9. Distribution of station data in the Semiarid Southwest region for: (a) 1-hour; and (b) 24-hour index flood intensities.

(a)

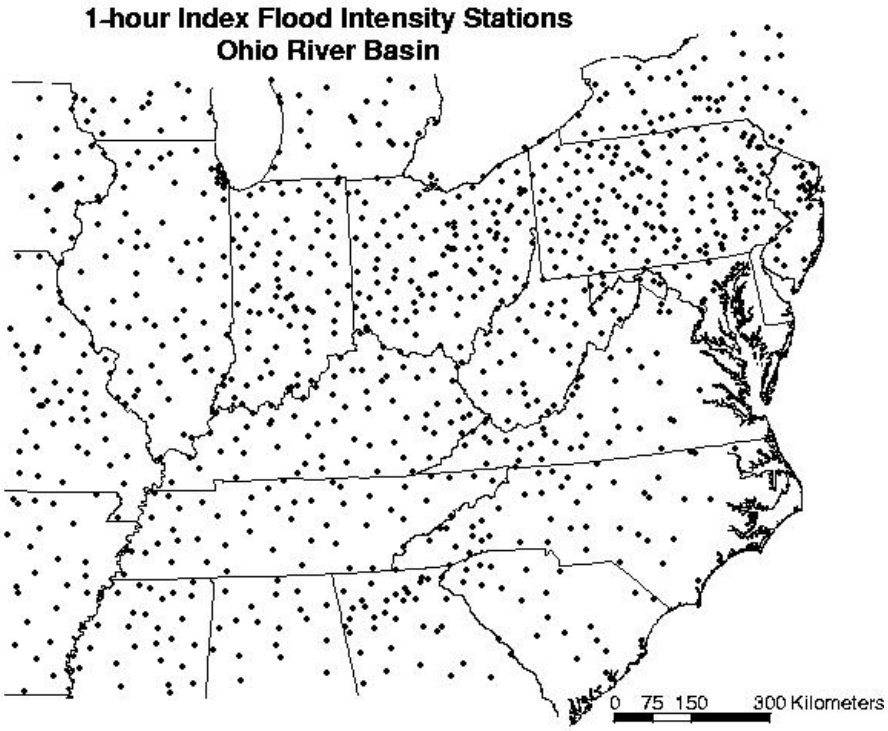

(b)

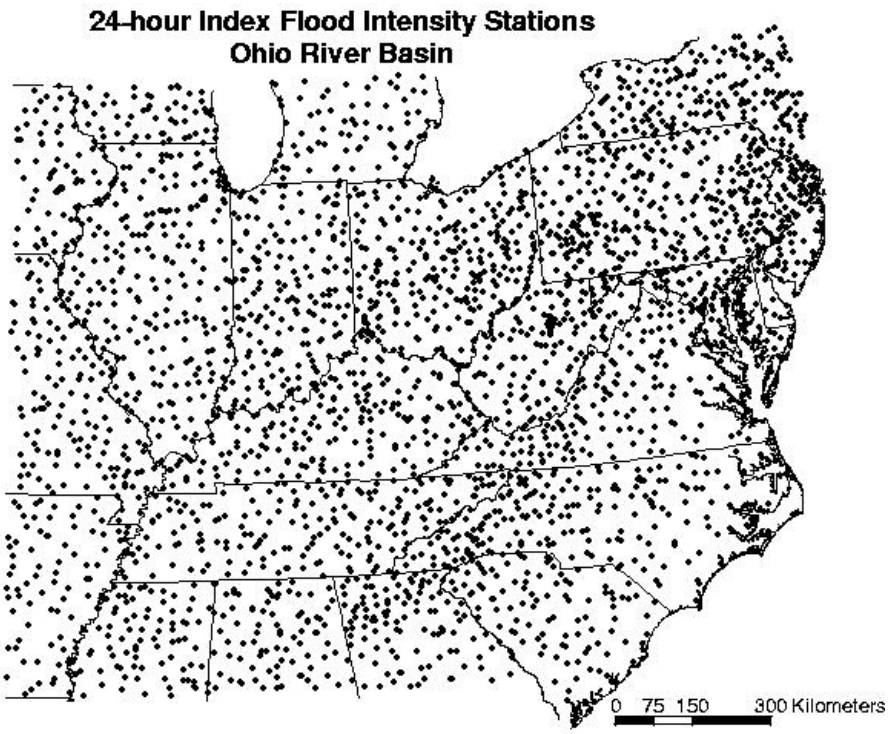

Figure 10. Distribution of station data in the Ohio River Basin for: (a) 1-hour; and (b) 24-hour index flood intensities.

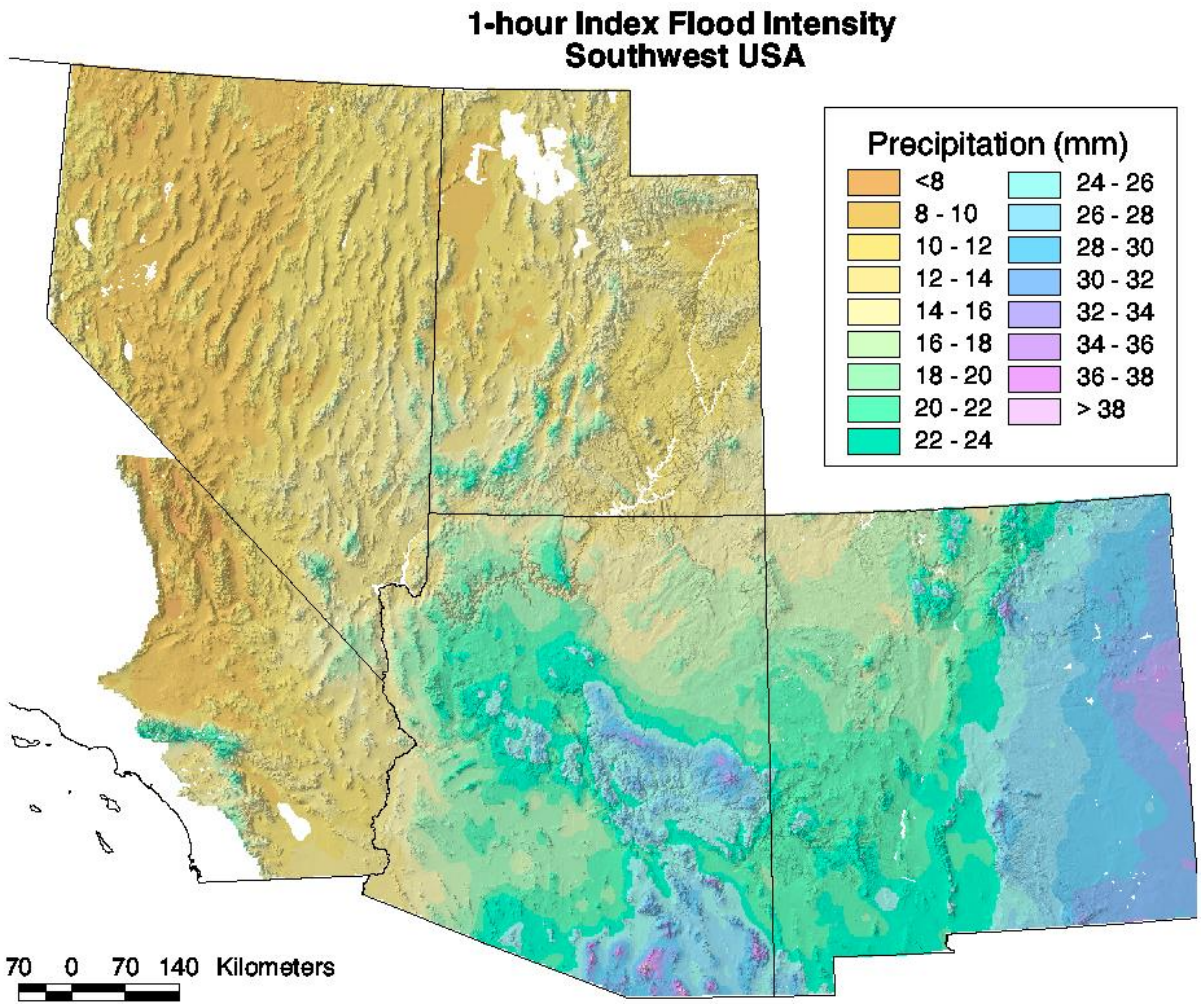

Figure 11. Final PRISM grid of 1-hour all-season, index flood intensity for the Semiarid Southwest region.

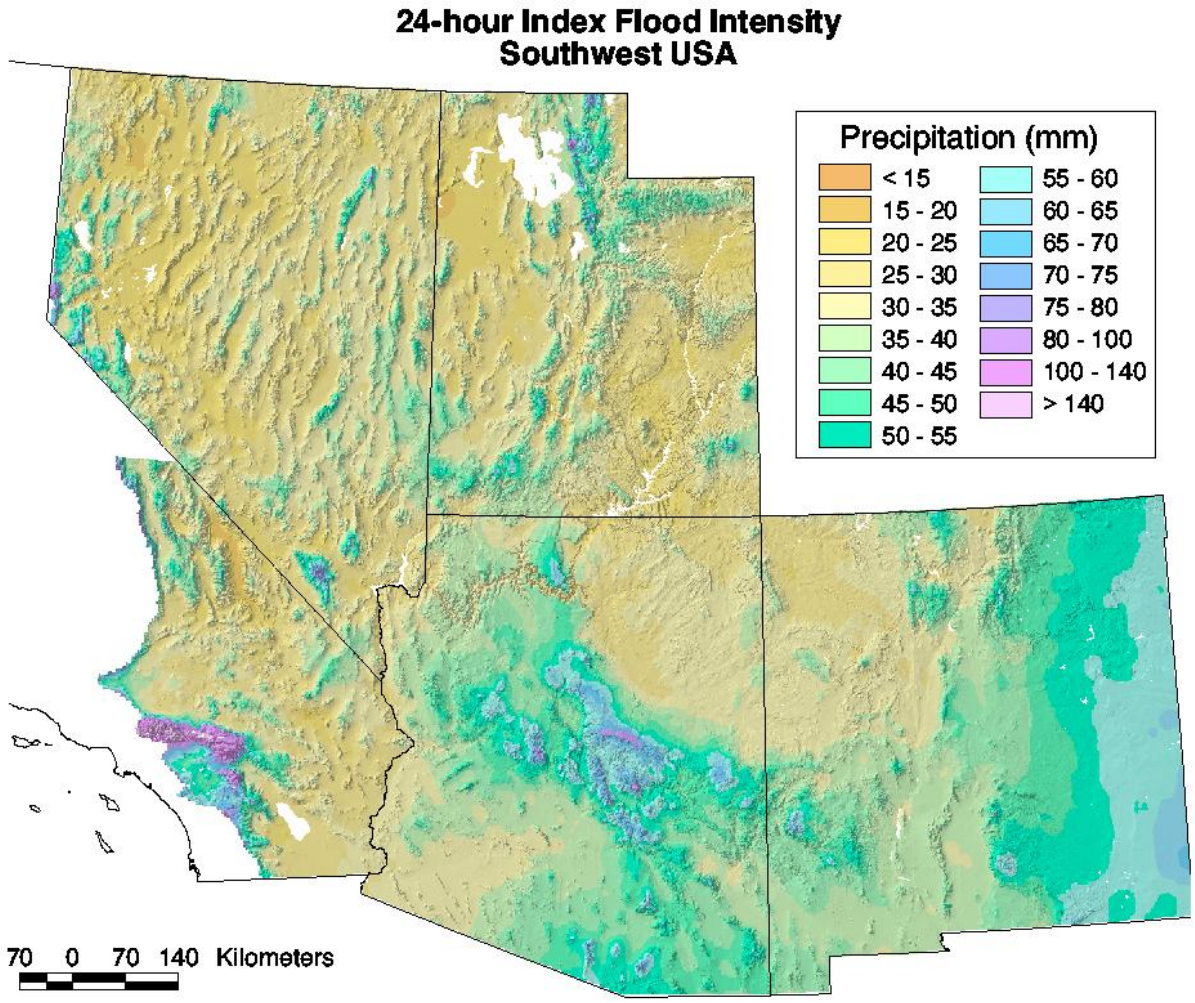

Figure 12. Final PRISM grid of 24-hour, all-season, index flood intensity for the Semiarid Southwest region.

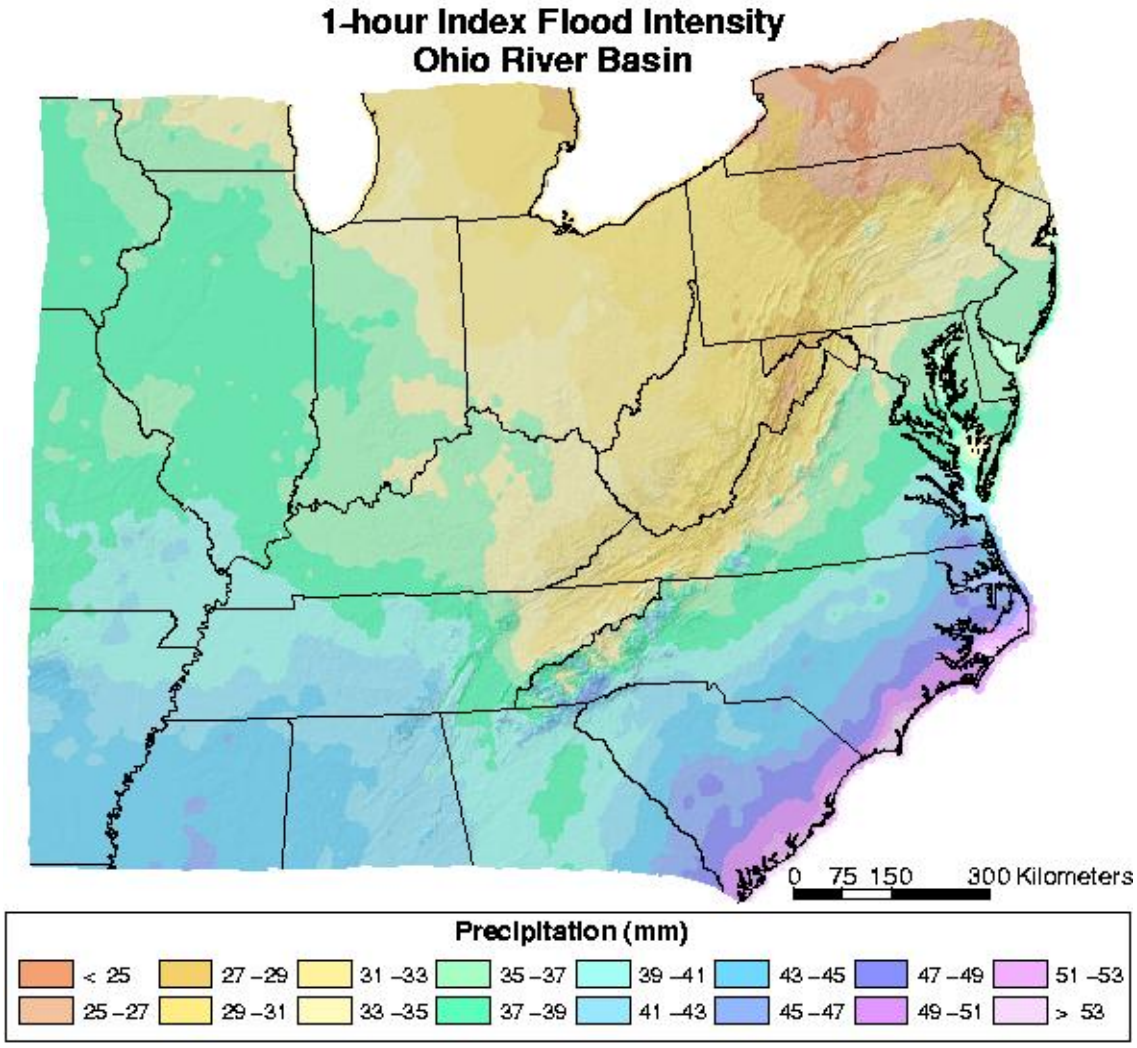

Figure 13. Final PRISM grid of 1-hour all-season, index flood intensity for the Ohio River Basin.

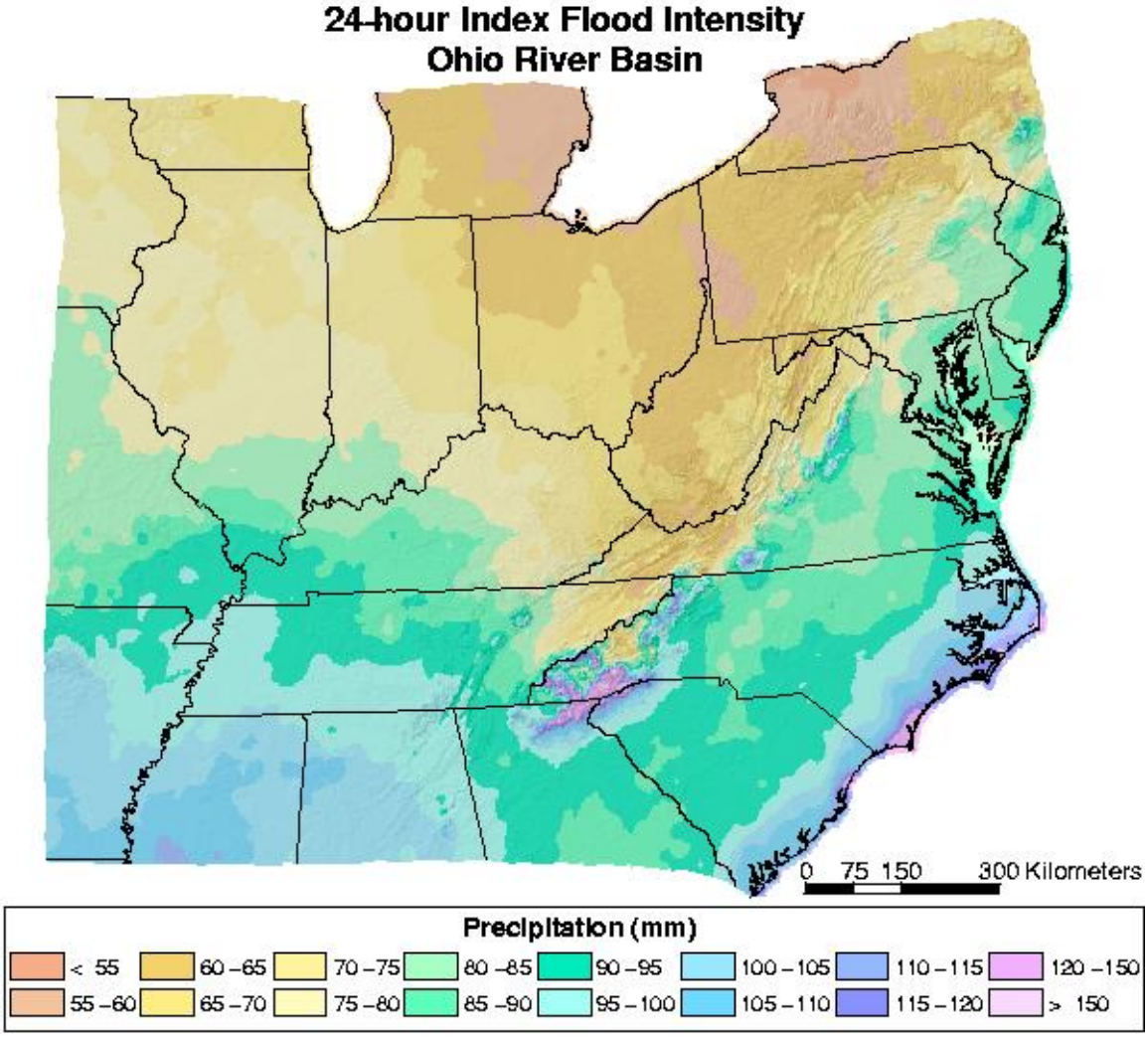

Figure 14. Final PRISM grid of 24-hour all-season, index flood intensity for the Ohio River Basin.